4.8 HIGH-HEAT FLUX TESTING OF LOW-LEVEL IRRADIATED MATERIALS USING PLASMA ARC LAMPS — A.S. Sabau, Y. Katoh, and Sarma Gorti (Oak Ridge National Laboratory)

OBJECTIVE

The objective of this work, part of the PHENIX collaboration with Japan, is testing of irradiated candidate divertor component materials and mock-up divertor components under high-heat flux conditions using Plasma Arc Lamps (PAL).

SUMMARY

In this reporting period, a simplified thermo-mechanical model was developed and implemented in ABAQUS™ in order to understand the deformation and residual stresses in the samples tested under high-heat flux. The results of the thermo-mechanical model simulations indicated that W/F82H specimens tested at high-heat fluxes expected in fusion power devices would deform plastically and undergo complex deformation states. The numerical simulation results for the stress levels and pattern of deformation are essential to the understanding of the property degradation and damage mechanisms during HHFT.

PROGRESS AND STATUS

Effort was conducted in three main areas: (a) analysis of data acquired during HHFT of five W-F82H specimens, (b) development of a simplified model for heat transfer during HHFT in order to estimate the thermal gradient through the specimen, and (c) development of a simplified thermo-mechanical model in ABAQUS for the simulation of the state of stress and deformation during HHFT.

First, the temperature data for the high-heat flux testing of five specimens, which was conducted in collaboration with Dr. Kazutoshi Tokunaga of Kyushu University, Japan in Dec. 2014, as part of the PHENIX program, were analyzed to formulate models for temperature evolution during HHFT. It was found that the average heat flux per cycle for each of the five specimens was above 210 W/cm^2 and did not vary significantly: 292.35, 253.52, 297.93, 297.24, and 295.21 W/cm^2, respectively. The main variables in the high-heat flux testing were the number of cycles at high heat flux and average cycle duration (Table 1).

Table 1. Main variables during HHFT.

Specimen	[2]No. Cycles	[2]Average cycle time [s]	Cycle duration [s]	Max. Heat Flux [W/cm^2]	Total heat input from PAL [MJ/cm^2]	Total heat input [MJ/cm^2]	Total time at high-heat flux [s]
1	119	12	10-15	300	0.476	0.418	1,428
2	172	8	7-10	210-278	0.369	0.349	1,375
3	226	4.73	4-5	300	0.338	0.318	1,069
[1]4	100	14.8	10-16	300	0.456	0.44	1,480
[1]5	54	13	10-15	300-323	0.242	0.207	702

[1] Specimen diameter 6 mm. Diameter was 10mm for specimens 1, 2, and 3.
[2] Number of cycles at heat fluxes above 210 W/cm^2.

Second, based on the analysis of the experimental data, several simplified modeling approaches were proposed in order to understand the deformation and residual stresses in the samples tested under high-heat flux. The specimen was bolted directly onto a Cu cooling rod to attain the lowest temperature on the back surface of the specimen and thus enabling the highest thermal gradient in the specimen (Figure 1a). As armor materials, such as W, are much stiffer than Cu, during HHFT, the specimen deformation would be imprinted into the Cu contacting surface. Thus, to ensure a reproducible contact between the armor specimen and Cu rod, a Cu washer was placed between the armor specimen and Cu rod. The

availability of accurate temperature data on the back surface of the Cu washer was essential to the development of the simplified thermal model. The accurate temperature measured on the back surface of the Cu washer was considered a known, an input quantity. This assumption enabled the calculation of the heat flux removed on the back surface of the Cu washer by water-cooling within the Cu rod. The simplified model heat transfer model eliminated the need for complex Computational Fluid Dynamics (CFD) simulation of the water flows and the coupling of CFD and stress analysis. In this model, the thermal contact conduction (TCC) between the F82H and Cu washer is an unknown as the only the top surface temperature could not be measured.

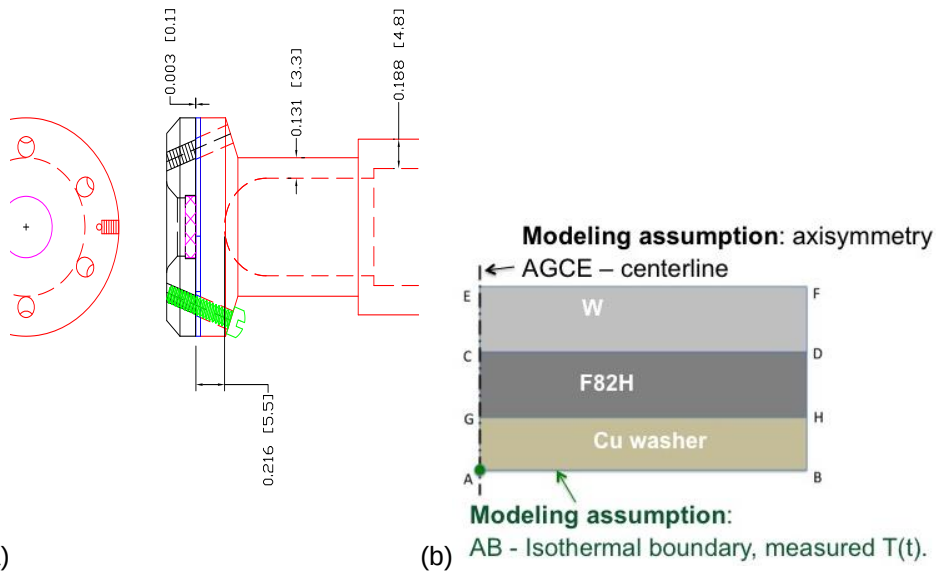

(a) (b)

Figure 1. Illustrations of the: (a) final design for the bolting fixture and cooling rod, and (b) main assumptions used to simply the thermal model during HHFT and actual model geometrical.

Third, in order to understand the deformation and residual stresses in the samples tested under high-heat flux, a coupled thermal and mechanical analysis is sought. Temperature-dependent mechanical properties for the materials involved were obtained in preparation for numerical simulations. Inelastic properties, including hardening properties, were obtained from open literature for F82H steel and Cu materials. From the stress-strain curves for F82H, the data for the hardening model was obtained. Thermomechanical models for the simulations of entire HHFT were implemented in the ABAQUS™ software.

Finally, the numerical simulation results were conducted for sample S5. The actual high-temperature cycles for specimen S5 are shown in Table 2. The duration from the end of each cycle to the onset of the next high-heat flux cycle was approximately 70-100s. The main modeling assumptions are illustrated in Figure 1 and Figure 2 and include: (1) modeling of the specimen (W-F82H) and Cu washer below it, (2) isothermal boundary condition at the back surface of the Cu washer, as prescribed by the actual measured temperature during HHFT, and (3) a rigid body clamp, i.e., keeping the distance between the clamp surface to the back-side of the Cu washer constant.

Table 2. High-heat flux cycles experienced by specimen S5.

Cycles	Heat Flux [MW/m^2]	Duration [s]
1-6	0.987	10
7-12	1.194	10
13-18	1.41	10
19-24	1.41	12
25-30	1.41	15
31-36	1.41	20
37-42	1.5	10

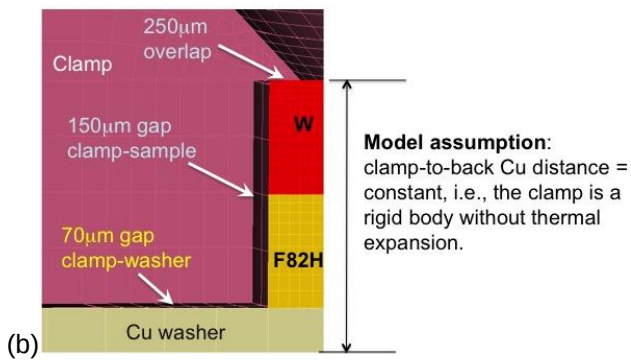

(b)

Figure 2. Illustrations of the clamping detail and rigid body assumption of the clamping fixture.

For the last HHFT cycle, the calculated temperatures at the top surface of W, top and back surfaces of F82H, and top of Cu washer are shown in Figure 2. The results presented were for thermal contact conduction (TCC) per unit area (between the F82H and Cu washer) of 5,000 and 7,000 [W/m^{2}K].

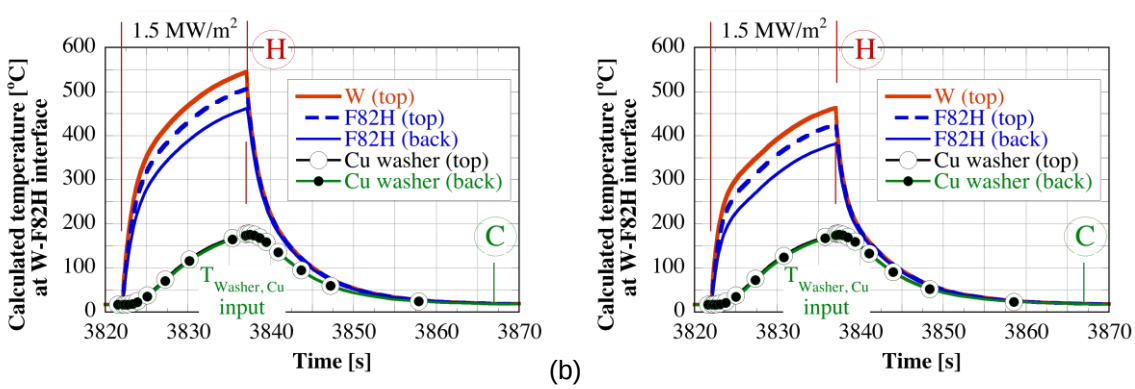

Figure 3. Calculated temperature evolution during cycle 42 for thermal contact conduction per unit area between the F82H and Cu washer of (a) 5,000 and (b) 7,000 [W/m^{2}K]. The temperature on the back-surface of the Cu washer was used as input.

Based on the temperature and mechanical properties, the following variables were calculated: specimen deformation, plastic deformation, and build-up of residual stresses during HHFT. The results for the Von Mises stress [Pa] is shown at two instances for cycle 42, as indicated by letters H and C in Figure 3. At

these instances, the specimen is at high temperature (Hot), i.e., right at the end of the HHF, and at room temperature (Cold), respectively. The stresses are shown on a deformed mesh in order to illustrate the changes in the specimen geometry during HHFT, with the deformation scale indicated in figures. Figure 4 and Figure 5 contain the data for the case when TCC would be 5,000 and 7,000 [W/m^{2}K], respectively. Although the specimen S5 was 6 mm, simulation data was also obtained for 10 mm specimens. The following observations can be made with respect to the stress and deformation results:

- At high temperatures, the specimens bulge *downward* at its center, as it is resting on the clamp at its outer edges,
- At room temperature, before clamp removal, the specimens bulge *upward* at its center,
- Predicted residual stresses after cooling are higher for the 6 mm than those for the 10 mm specimens.
- The maximum stress is predicted to occur in the steel, at the steel-W interface. The location of maximum stress is (a) at the edge of the steel for the 6 mm specimens, and (b) within the steel for the 10 mm specimens.

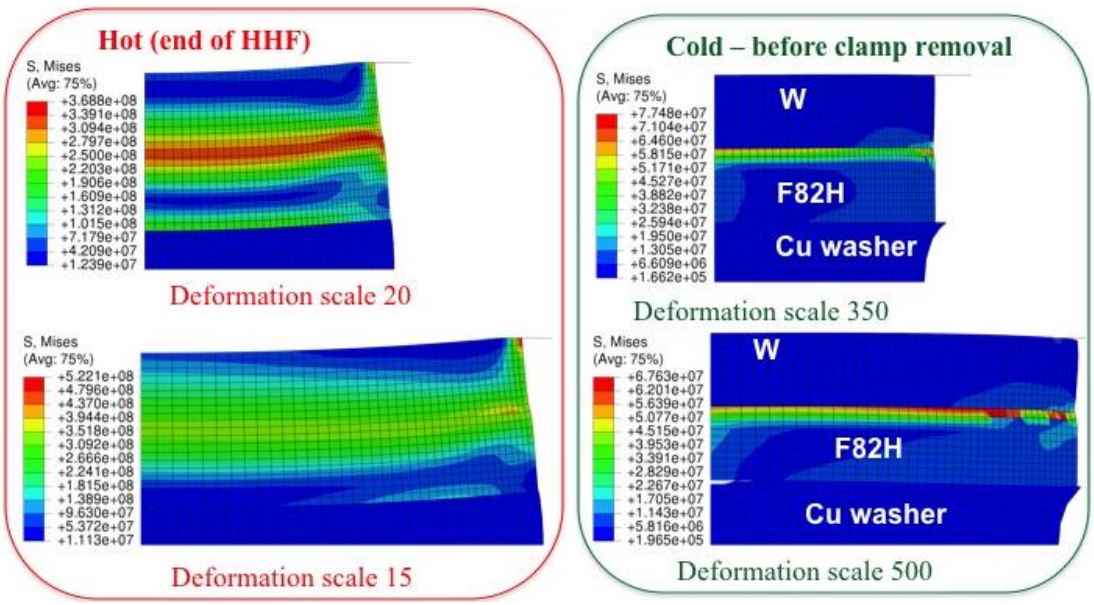

Figure 4. Von Mises stress results when specimen is at high temperature (Hot), i.e., right at the end of the HHF, and at room temperature (Cold) for 6 mm specimens (top line of figures) and 10 mm specimens (the last line of figures) for the case when TCC per unit area F82H-Cu was 5,000 [W/m^{2}K].

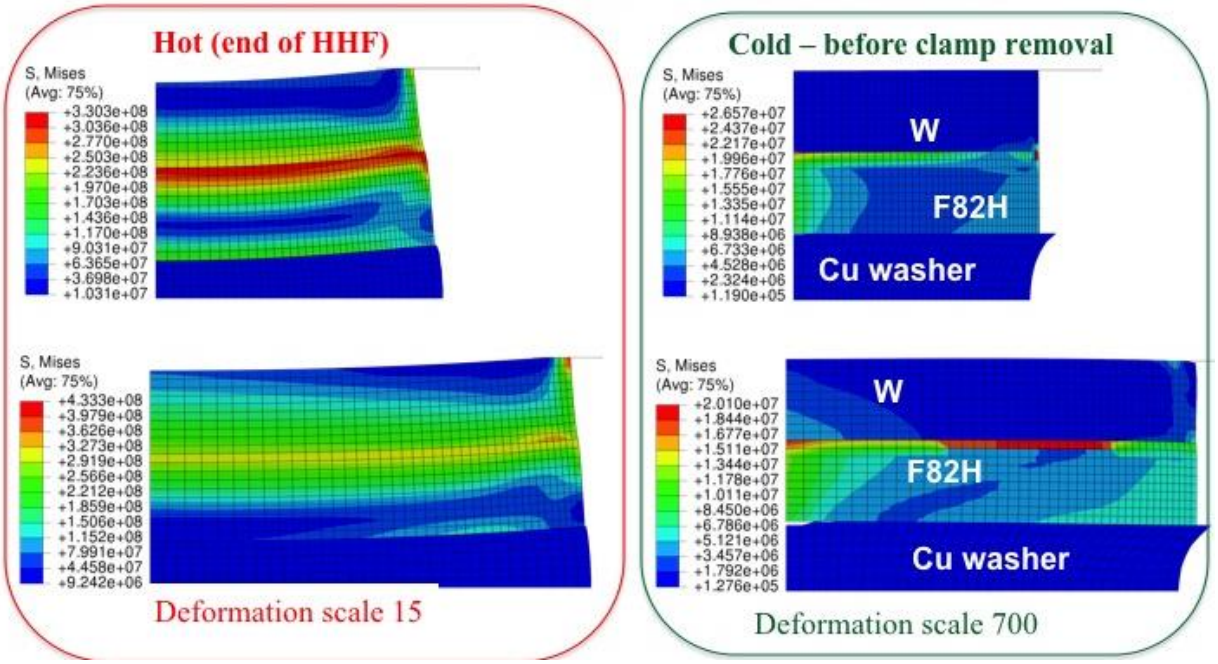

Figure 5. Von Mises stress [Pa] results when specimen is at high temperature (Hot), i.e., right at the end of the HHF, and at room temperature (Cold) for 6 mm specimens (top line of figures) and 10 mm specimens (the last line of figures) for the case when TCC per unit area F82H-Cu was 7,000 [W/m^{2}K].